Research Article | Vol. 14, No. 6 / 1 Jun 2023 / Biomedical Optics Express 2857
Biomedical Optics EXPRESS

Laser pulse train parameters determine the brightness of a two-photon stimulus

MARCIN J. MARZEJON,[1,2,3] ŁUKASZ KORNASZEWSKI,[1,2] MACIEJ WOJTKOWSKI,[1,2] AND KATARZYNA KOMAR[1,2,4,*]

[1]International Centre for Translational Eye Research, Skierniewicka 10a, 01-230 Warsaw, Poland
[2]Department of Physical Chemistry of Biological Systems, Institute of Physical Chemistry, Polish Academy of Sciences, M. Kasprzaka 44/52, 01-224 Warsaw, Poland
[3]Department of Metrology and Optoelectronics, Faculty of Electronics, Telecommunications and Informatics, Gdańsk University of Technology, G. Narutowicza 11/12, 80-233 Gdańsk, Poland
[4]Institute of Physics, Faculty of Physics, Astronomy and Informatics, Nicolaus Copernicus University in Torun, Grudziądzka 5, 87-100 Toruń, Poland
*kkomar@fizyka.umk.pl

Abstract: This report presents the results of measurements of the two-photon vision threshold for various pulse trains. We employed three pulsed near-infrared lasers and pulse stretchers to obtain variations of the pulse duty cycle parameter over three orders of magnitude. We proposed and extensively described a mathematical model that combines the laser parameters with the visual threshold value. The presented methodology enables one to predict the visual threshold value for a two-photon stimulus for a healthy subject while using a laser source of known parameters. Our findings would be of value to laser engineers and the community interested in nonlinear visual perception.

1. Introduction

Humans can perceive electromagnetic radiation from 380 nm to 780 nm, called visible light [1]. In some circumstances, both shorter [2] and longer [3,4] wavelengths may be seen; but, in general, the human eye cannot perceive infrared radiation. However, it has been observed that a pulsed near-infrared (NIR) laser beam could be visible to an unaided human eye. The first known literature report was published by Vasilienko *et al.* in 1965 [5]. Various lines (948.6 nm, 1114.3 nm, 1117.7 nm, 1152.5 nm, and 1179.0 nm) of the Ne-H_2 gas laser emission (pulse duration of 5 µs) have been seen as color stimuli, corresponding to the half-wavelength counterparts of the laser emission wavelengths. Similar observations have been reported since that time [6,7]; but understanding of the phenomenon was unclear until it was thoroughly explained in 2014 by Palczewska *et al.* [8], who presented an extensive study, including experiments on mouse retinas, psychophysical measurements with humans, and biochemical and molecular modeling studies. They concluded that the perception of pulsed NIR laser beams is triggered by two-photon isomerization of the visual photopigments in the retina [8]. The nonlinear mechanism of vision has been named "two-photon vision" (2phV). The phenomenon of two-photon absorption in biological samples and tissues is not particularly surprising. However, the fact that it can occur in human visual pigments under safe conditions (*i.e.*, at power levels even 200 times below the safety limit for 60 min of continuous illumination of one retinal spot [9]) and trigger a visual sensation was truly unexpected.

This two-photon vision phenomenon has been studied so far mainly by using femtosecond lasers [10–13], which enable one to obtain a power-density level high enough for the two-photon absorption to occur. It should be emphasized that such an approach is reasonable for experimental setups in optical laboratories, but not particularly convenient to apply in a real-life application; *e.g.*, a two-photon microperimeter in an ophthalmic clinic [12]. Therefore, new light sources for

#489890 https://doi.org/10.1364/BOE.489890
Journal © 2023 Received 17 Mar 2023; revised 21 Apr 2023; accepted 28 Apr 2023; published 24 May 2023

Biomedical Optics EXPRESS

the two-photon vision phenomenon were sought. In 2019, Ruminski *et al.* were the first to attempt to characterize the change in visual threshold while increasing pulse duration [14]. In their experiment, the pulses from a femtosecond laser (pulse duration of full-width at half maximum $\tau = 250$ fs, pulse repetition frequency $PRF = 63$ MHz) were stretched from 490 fs to about 10 ps using the dispersion of an optical fiber. The authors estimated the pulse duration based on the length of the optical fiber (which varied from 1 m to 38 m). The measured visual sensitivity threshold did change with the change in pulse duration (3.6-fold increase between 490 fs and 10 ps pulses); but, surprisingly, the results of these psychophysical experiments did not agree with the theoretical predictions – a 4.5-fold change was expected [14]. In 2020, Manzanera *et al.* presented a study where visual threshold values were measured for a spectrally-filtered supercontinuum laser at two repetition rates (1.98 kHz and 9.91 kHz) [15]. In 2021, Marzejon *et al.* compared the relative efficiency for two-photon vision applications of a pulsed femtosecond laser ($\tau = 253$ fs, $PRF = 62.65$ MHz) *versus* a picosecond laser ($\tau = 12.2$ ps, $PRF = 19.17$ MHz) [9]. That study showed that the picosecond lasers could be applied successfully for two-photon perimetry, even though they were somewhat less perceived (around 3.9-times) by the volunteers [9]. In this case, the differences in the visual threshold values are explainable by the differences in the laser pulse train parameters and agree with the theoretical model presented in the paper. However, it must be emphasized that in both articles [14,20], only two pulse trains were investigated. In a subsequent conference paper, our research group reported an extended set of infrared pulse trains with picosecond pulses ($\tau = 2$ ps, $PRF = 62.65$ MHz) [16]; the results agreed with the modeling presented in [9].

Our current study compares the results of two-photon visual threshold measurements for various pulse trains. We employed three pulsed NIR-laser sources and pulse stretchers to obtain variation over three orders of magnitude of the pulse duty cycle parameter δ that is the product of the laser pulse duration τ and pulse repetition frequency *PRF*. All of the experimental factors regarding the pulsed stimulating laser were carefully measured and fully controlled during the psychophysical experiments. Moreover, we proposed and have extensively described a mathematical model that combines the pulse train parameters (pulse duration and pulse repetition frequency) with the visual threshold value. Herein we show that our experimental data agree with the model. The methodology and results enable one to predict the visual threshold value for a particular two-photon stimulus to a healthy subject, when using a laser source of known pulse train parameters and similar experimental conditions. As laser technology development has advanced, especially fiber-based lasers, the available range of pulse duration and pulse repetition frequency has significantly increased, so the results and conclusions reported herein have value both practically and theoretically. The interest of laser engineers is likely to be piqued, as modifications in the pulsed NIR-laser parameters enable them to be optimized for two-photon vision or retinal imaging applications (here, the perception of the laser beam is sometimes undesirable). This report also serves the research community interested in nonlinear visual perception. Our work may contribute also to the development of either two-photon vision-based ophthalmic devices or a new generation of two-photon driven displays (*e.g.*, retinal projectors), which are emerging as interesting tools for virtual reality (VR) and augmented reality (AR) applications.

2. Methods

This Section describes the methods used for the visual threshold measurements. Section 2.1 describes the experimental setup, Section 2.2 focuses on the psychophysical testing procedure, and Section 2.3 provides the mathematical model that connects the two-photon visual threshold with the parameters of a laser source.

Biomedical Optics EXPRESS

2.1. Experimental setup

The two-photon visual thresholds were measured using a laboratory optical set-up with a functionality of perimeter, presented in Fig. 1 a) and described in detail in our previous work [9]. Briefly, the stimulating laser beam, indicated in Fig. 1 a) with a green line, is shaped into a stimulus with galvanometric scanners GSC (GVS002, Thorlabs), reflected on beamsplitter BS_2, and displayed onto a specified retinal position of the subject's eye. GSC are optically conjugated with the eye pupil plane by the telescope L_3-L_4. A moveable lens L_3 enables compensation of the refractive error of the subject's eye. The optical power of the beam corresponding to the stimulus brightness is controlled by a gradient filter GF (NDC-50C-4, Thorlabs, 0÷4.0 variable optical density) steered by a stepper motor SM (ST4209X1004-A, Nanotec, 1/64 step operating mode). Part of the beam is deflected by the beamsplitter BS_1 (50:50) to continuously monitor the power level with the power meter sensor PM (S120C, Thorlabs, measurement uncertainty ±7%). The relationship between the optical power at the eye pupil plane and the power meter sensor PM readings was established before each round of measurements by power measurements with an additional sensor (S120C or S121C, Thorlabs, measurement uncertainty ±7%) placed in the pupil plane, at the output of the system. The measurements with both sensors were performed simultaneously for the entire available range of stimulating beam powers. The beam attenuation coefficient between the PM sensor and the pupil plane was determined by linear regression.

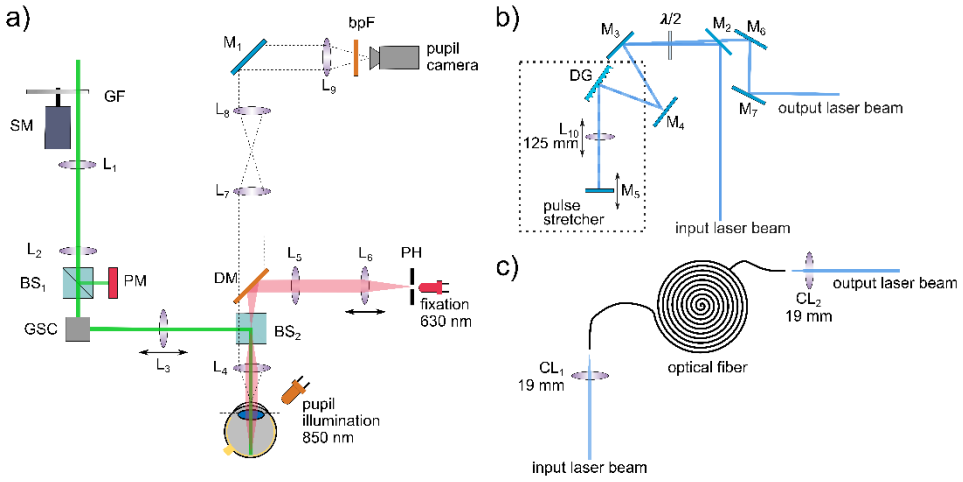

Fig. 1. Optical diagrams of the employed systems. a) General optical diagram of the two-photon perimeter. b) Optical diagram of the diffraction grating-based (Martinez-type) pulse stretcher. c) Optical diagram of the fiber-based pulse stretcher. Definitions: bpF – bandpass filter; BS_i – beamsplitter; CL_i – collimating lens; DG – diffraction grating; DM – dichroic mirror; GF – neutral density gradient filter; GSC – xy galvanometric scanners; λ/2 – half-wave plate; L_i – lens; M_i – mirror; PH – pinhole; PM – power meter head; SM – stepper motor.

The perimeter has two features that improve the eye position stability during the psychophysical experiments – a fixation point and a pupillary camera. The optical paths of the fixation point and the pupillary camera were combined with the stimulating beam path by the beamsplitter BS_2. The fixation point is a faint red dot at the center of the visual field, optically conjugated with the retinal plane. The subject was asked to fix their eye on that point during measurements. The movable lens L_6 was used for compensate refraction for the fixation dot, independently of the stimulus, which prevented longitudinal chromatic aberration in the eye. The pupillary camera (DCC1545M, Thorlabs) enabled the preview of the eye position during the test, and continuously

Biomedical Optics EXPRESS

adjustment of the subject's head position by the operator, if needed, based on this preview. For that purpose, the eye was illuminated with an infrared pupil illuminator (central wavelength of 850 nm, spectral width at width at half maximum of 30 nm). During the measurement, pupillary camera images were recorded for reference in post-processing, the methods used for image analysis were described in [9,10]. The analysis revealed that approximately in half of the trials, the beam's average distance from the pupil's center did not exceed 0.5 mm. For the other half of the cases, this distance was twice as large, but still less than 1 mm. According to [17], changes in beam intensity caused by the Stiles-Crawford effect can be considered negligibly small.

The stimulating beam originated from one of three pulsed-NIR lasers: a solid-state sub-picosecond laser HighQ-2 by Spectra-Physics, called *fs laser*; a fiber-optics picosecond laser Jive by Fluence, called *ps laser*; or a spectrally-shifted frequency-doubled femtosecond Er-doped fiber laser described in [11], called *tunable fs laser*. The central wavelength of the latter was set to 1042 nm for psychophysical experiments. The parameters of the laser sources are summarized in the Table 1. All the laser sources emitted NIR radiation in a similar wavelength range but were different in terms of pulse duration and repetition frequency.

Table 1. Parameters of laser sources employed for psychophysical tests. Definitions: λ_c – central wavelength; $\Delta\lambda$ – spectral full width at half maximum; τ – pulse at full width at half maximum; *PRF* – pulse repetition frequency.

Laser source	λ_c [nm]	$\Delta\lambda$ [nm]	τ [ps]	*PRF* [MHz]
fs laser	1043.3	4.8	0.253	62.65
ps laser	1028.4	12.5	12.2	19.17
tunable fs laser	1042.1	9.9	0.197	51.5

To obtain more variability of the duration of the laser pulse, the pulses of the *fs laser* and the *ps laser* were stretched with a grating-based (Martinez-type) or optical fiber-based pulse stretcher. The optical diagrams of the stretchers are presented in Fig. 1 b) and 1 c), respectively. Pulse stretching with a grating-based stretcher is described in our previous work [16]. Briefly, the laser beam was steered onto a reflective diffraction grating DG (GR25-1210, Thorlabs) with the mirrors M_2-M_4. The deflected 1st order beam passed through the lens L_{10} and was reflected from the mirror M_5. After the reflection from M_5, the beam passed again through the lens L_{10}, was deflected from the diffraction grating DG, and was steered onto the apparatus by the mirrors M_3-M_4 and M_6-M_7. The 1st order diffraction efficiency was optimized by a half-wave plate $\lambda/2$ (AHWP10M-980, Thorlabs), placed in front of the diffraction grating.

The optical fiber-based stretcher used the pulse elongation caused by the chromatic dispersion of an optical fiber. It consists of an optical fiber (HI 780, Corning) and two lenses: CL_1, which introduces the beam into the optical fiber, and CL_2, which collimates the output beam. The pulse elongation was obtained by modifying the power of the incident laser beam and the optical fiber length (100 m or 1 km). The parameters of the pulse trains used in the psychophysical experiments are presented in Table 2. The details concerning the pulse duration and spectrum measurements are presented in Section S1 of the Supplementary Information.

2.2. Psychophysical testing

The psychophysical experiments were performed with twenty-one healthy subjects with normal or corrected-to-normal vision and no history of ocular diseases. The average age of the tested group was 31.6 years (21 to 47 years; distribution shown in Fig. 2 a). Each volunteer was dark-adapted for 30 min before the experiments in a dark room (<0.01 lux), and their pupils were dilated and accommodation paralyzed with two drops of Tropicamide 1%. The two-photon absorption efficiency depends strongly on power density at the retina. Reduction of accommodation amplitude caused by Tropicamide drops also reduces fluctuations of the two-photon visual

Biomedical Optics EXPRESS

Table 2. Parameters of laser pulse trains employed for psychophysical tests. Definitions: GBS – grating-based pulse stretcher; FBS – fiber-based pulse stretcher; τ – pulse duration at full width at half maximum; *PRF* – pulse repetition frequency; δ – duty cycle; λ_c – central wavelength, the fiber length is indicated; $\Delta\lambda$ – spectral full width at half maximum; D – beam diameter ($1/e^2$) at the pupil plane (for elliptical beams, both axis sizes are provided); N – number of tested subjects.

Laser source	Modification	τ [ps]	*PRF* [MHz]	δ	λ_c [nm]	$\Delta\lambda$ [nm]	D [mm]	N
tunable fs laser	——	0.197	51.5	1.01×10^{-5}	1042.1	9.9	2.1×1.4	4
fs laser	——	0.253	62.65	1.58×10^{-5}	1043.3	4.8	1.5	15
fs laser	GBS	2	62.65	1.25×10^{-4}	1043.3	5.3	1.2×1.6	8
ps laser	——	12.2	19.17	2.34×10^{-4}	1028.4	12.5	2.1	15
fs laser	FBS (100 m)	44.9	62.65	2.81×10^{-3}	1043.3	10.3	1.85	4
ps laser	FBS (1 km)	92.4	19.17	1.77×10^{-3}	1029.3	7.5	2.0	4
fs laser	FBS (100 m)	269	62.65	1.69×10^{-2}	1043.3	18.4	1.6	4
fs laser	FBS (1 km)	759	62.65	4.70×10^{-2}	1043.3	6.8	1.6	3

threshold caused by different focusing on the retina. All tests were performed after obtaining written informed consent. All the procedures complied with the Declaration of Helsinki and ANSI Z136:2014 standards [18], and were approved by the Ethics Committee of the Collegium Medicum, Nicolaus Copernicus University in Toruń.

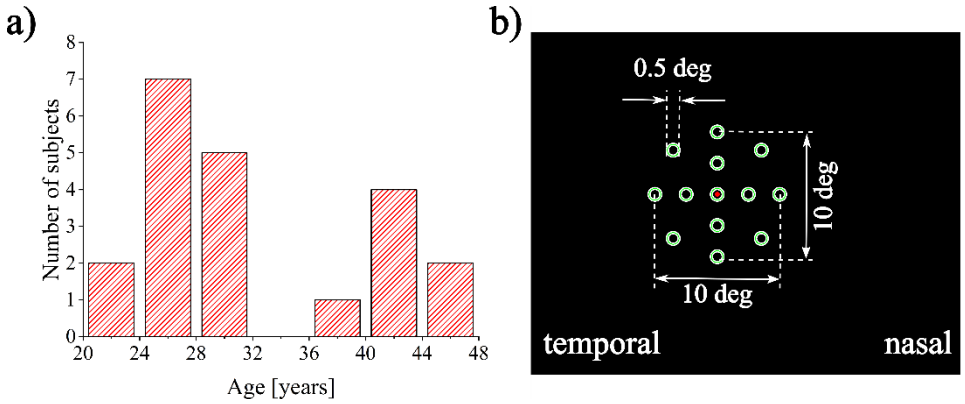

Fig. 2. Psychophysical testing. a) Age distribution of the subjects. b) Grid of tested retinal locations. The greenish circles and the red dot correspond to the investigated retinal locations and the position of the fixation point, respectively.

The two-photon visual threshold was found with the so-called 4-2-1 threshold-finding strategy. The algorithm and its implementation are described in our previous work [9]. The stimulus was a 0.5-deg diameter (Goldmann III) flickering ring (0.2s ON, 0.6 s OFF, 100 Hz scanning repetition rate). For each subject, the visual threshold value measurement was performed once at a given retinal location. The testing of 13 retinal locations (up to ±5 deg foveal eccentricity; see Fig. 2 b)) took 5 to 7 min.

The Maximum Radiant Power (MPΦ) level at the pupil plane used during the experiments did not exceed 800 µW, which corresponds to the Maximum Permissible Radiant Power level for 5 min-long exposure to a stationary beam, calculated based on the ANSI standard [18] (see Section S2 of Supplementary Information). It is worth mentioning that during the psychophysical experiments, a single retinal spot is being illuminated for a much shorter time due to: (1) flickering stimulus; (2) ring stimulus instead of a stationary beam; (3) various retinal locations

Biomedical Optics EXPRESS

investigated during the test; and (4) examination time of 5-7 min. These facts ensured that the experiment was safe. different

2.3. Mathematical model

Two-photon vision (2phV) is based on a nonlinear optical mechanism: two-photon absorption by the chromophores in the retina [8]. Based on Xu *et al.* [19], we associated the measured visual threshold power level for the two-photon vision with various duty cycles of the laser pulse trains.

For the two-photon absorption process, the number of absorbed photons per unit of time $N_{2p}(t)$ may be described by the following formula [19]:

$$N_{2p}(t) = \int_V C(r,t) I^2(r,t) \sigma_{2p} dV, \tag{1}$$

where $C(r, t)$ is the concentration of the absorbing molecules, $I(r, t)$ is the incident light intensity, σ_{2p} is the two-photon absorption cross-section, and V is the illuminated volume. Assuming no photobleaching or saturation of the absorbing molecules, as expected for the conditions of absolute visual threshold measurement, the concentration $C(r, t)$ does not change over time. We assume here that changes in concentration of 11-cis retinal caused by our stimulus are negligibly small because (1) we're operating at powers close to the visual threshold, so the number of isomerized molecules is small in comparison to the entire pool of available molecules, (2) our scanning beam forms stimulus in the shape of the thin ring, thus it doesn't hit exactly the same photoreceptors with every repetition of the scanned frame - the eye movements distribute the light across the retinal mosaic. Therefore, we will focus on the incident light intensity term $I(r, t)$ that is a product of the spatial (unitless) distribution of the incident light $S(r)$ and the light intensity $I_0(t)$ (see Eqs. (2) and (8) in [19]). The spatial distribution of the incident light $S(r)$ corresponds to the intensity-normalized point spread function for a diffraction-limited lens. The light intensity at the geometrical focal point $I_0(t)$ is strictly connected with the instantaneous optical power $P(t)$ of the incident light beam [19] (see Eq. (9) in [19]):

$$I_0(t) = \frac{\pi (NA)^2}{\lambda^2} P(t), \tag{2}$$

where NA is the numerical aperture, and λ is the wavelength of the illuminating light. Taking into account the eye medium transmittance $T(\lambda)$ and applying the paraxial approximation, Eq. (2) may be rewritten as follows [15,19]:

$$I_0(t) = T(\lambda) \frac{\pi}{\lambda^2} \left(\frac{D}{2 f_{eye}} \right)^2 P(t), \tag{3}$$

where D is the diameter of the stimulating beam size, and f_{eye} is the focal length of the human eye (equal to 17 mm following the Gullstrand eye model [20]). For a pulsed laser, the overall optical power delivered to the retina is equal to the optical power of a single pulse multiplied by the number of light pulses:

$$\langle P \rangle = t_{\text{exp}} PRF \int_{-t_1}^{t_1} P_{\text{pulse}}(t) dt, \tag{4}$$

where t_{exp} is the total exposure time on pulsed laser radiation, PRF is the laser pulse repetition frequency, t_1 is the integration time, $t_1 = 2/PRF_1$, and $P_{pulse}(t)$ is the optical power of a single laser pulse. The optical power of a simple laser pulse can be described either as a gaussian

Biomedical Optics EXPRESS

distribution:

$$P_{pulse,gaussian}(t) = P_{max} exp\left[-4\ln 2\left(\frac{t-t_0}{\tau}\right)^2\right] \tag{5}$$

or a sech^2 distribution:

$$P_{pulse,sech^2}(t) = P_{max} \cdot sech^2\left(1.76 \cdot \frac{t-t_0}{\tau}\right) \tag{6}$$

of amplitude P_{max}, centered at the time $t_0 = 0$, and the width corresponds to the full-width at half-maximum (FWHM) pulse duration τ.

For the two-photon absorption process, two photons per excited molecule are utilized. The number of excited photopigment molecules may be expressed as [19]:

$$N^*_{2p}(t) = \frac{1}{2}\phi_{2p} C \sigma_{2p} I_0^2(t) \tag{7}$$

where ϕ_{2p} is the two-photon absorption quantum efficiency. Equation (7) expresses the instantaneous number of excited photopigment molecules. In fact, the visual sensation depends on a time-averaged number of excited photopigment molecules (see Eq. (4) in [19]):

$$\left\langle N^*_{2p}(t)\right\rangle = \frac{1}{2}\phi_{2p}\sigma_{2p}T(\lambda)^2\left(\frac{\pi}{\lambda^2}\right)^2 \int_V C(r)S^2(r)dV\left(\frac{D}{2f_{\text{eye}}}\right)^4 t_{\text{exp}} PRF \int_{-t_1}^{t_1} P^2_{pulse}(t)dt \tag{8}$$

which can be simplified to:

$$\langle N^*_{2p}(t)\rangle = K_m K_b t_{exp} PRF \int_{-t_1}^{t_1} P^2_{pulse}(t)dt, \tag{9}$$

where K_m is a constant related to the medium, and K_b is a constant related to the laser beam geometry [9]. Note that comparing the number of absorbed photons for the same sample and for laser sources of the same spectral properties under the same conditions (numerical aperture, exposure time), the difference in the number of absorbed photons is dependent only on the laser pulse repetition frequency and the laser pulse power.

As the two-photon absorption process triggers the two-photon vision [8], the same number of excited molecules (or absorbed photons) is required to activate the 11-*cis*-retinal in the chromophores, despite the pulse train parameters (for the exact same illumination wavelength). This may be expressed as:

$$\langle N^*_{2p,1}(t)\rangle = \langle N^*_{2p,2}(t)\rangle, \tag{10}$$

where indices 1 and 2 correspond to the different pulse trains. Under the assumption that the retina is stimulated with two different pulsed lasers that differ only in terms of the pulse train parameters (pulse duration, pulse repetition frequency, or pulse shape), Eq. (1)0 takes the following form:

$$PRF_1 \int_{-t_1}^{t_1} P^2_{pulse,1}(t)dt = PRF_2 \int_{-t_2}^{t_2} P^2_{pulse,2}(t)dt, \tag{11}$$

and after further transformation:

$$PRF_1 \cdot \tau_1 \cdot P^2_{max,1} \cdot E_1 = PRF_2 \cdot \tau_2 \cdot P^2_{max,2} \cdot E_2, \tag{12}$$

where E_i is equal to:

$$E_{i,\ gaussian} = \frac{1}{2} \cdot \sqrt{\frac{\pi}{\ln 4}} \cdot erf\left(\frac{4\ln 4}{\tau_i PRF_i}\right), \tag{13}$$

for a gaussian pulse (erf is an error function [21]), and

$$E_{i,\ sech^2} = -\frac{2}{3\cdot 1.76} \cdot tanh\left(\frac{3.52}{\tau_i PRF_i}\right)\left[tanh^2\left(\frac{3.52}{\tau_i PRF_i}\right) - 3\right], \tag{14}$$

for a sech^2 pulse. Equations (5) and (6) show that the information of the single pulse power $P_{pulse}(t)$ can be determined if amplitude P_{max} and pulse duration τ are known. As two (or more)

Biomedical Optics EXPRESS

pulse trains are compared, the ratio of the amplitudes is sufficient to determine the differences in visual threshold values for different duty cycle values. Based on Eq. (12), the ratio of the pulse amplitudes A_{2p} equals:

$$A_{2p} = \frac{P_{max,\,1}}{P_{max,2}} = \sqrt{\frac{\tau_2 PRF_2}{\tau_1 PRF_1}} \cdot \sqrt{\frac{E_2}{E_1}} = \sqrt{\frac{\delta_2}{\delta_1}} \cdot \sqrt{\frac{E_2}{E_1}}. \tag{15}$$

For both pulse shapes, the ratio of the amplitudes of the comparing pulse trains depends on the square root of the ratio of the laser duty cycle values. It is worth noting that for gaussian and sech^2-shaped pulses of the duty cycle values, that were used in the experiments described in this paper, the ratio of the erf and/or hyperbolic tangent terms are close to 1 (see Tables S2 and S3 in supplement part S3), and the pulse amplitude ratio depends mainly on the root of the ratio of the laser duty cycle values. This conclusion agrees with previous findings [9,15,16]. We would like to emphasize that the model presented here is extended compared to that of Manzanera *et al.* (see Eq. (11) in [15]), as it takes into account not only the influence of the pulse repetition frequency but also pulse duration and pulse shape.

Equation (15) expresses the ratio of the pulse amplitudes P_{max} of two pulse trains. However, a physical quantity that can be easily measured during the experiments is the mean optical power level at the threshold P. Comparing two different pulse trains, the expected mean power ratio R equals to:

$$R = \frac{\langle P_1 \rangle}{\langle P_2 \rangle} = \frac{t_{exp} \cdot PRF_1 \cdot \int_{-t_1}^{t_1} P_{pulse,1}(t)dt}{t_{exp} \cdot PRF_2 \cdot \int_{-t_2}^{t_2} P_{pulse,2}(t)dt} = \sqrt{\frac{\tau_1 PRF_1}{\tau_2 PRF_2}} \cdot \sqrt{\frac{E_2}{E_1}} \cdot \frac{F_1}{F_2} = \sqrt{\frac{\delta_1}{\delta_2}} \cdot \sqrt{\frac{E_2}{E_1}} \cdot \frac{F_1}{F_2}, \tag{16}$$

where F_i equals to:

$$F_{i,\,gaussian} = \frac{1}{2} \cdot \sqrt{\frac{\pi}{\ln 2}} \cdot erf\left(\frac{4 \ln 2}{\tau_i PRF_i}\right) \tag{17}$$

for a gaussian pulse, and to:

$$F_{i,sech^2} = \frac{2}{1.76} \cdot tanh\left(\frac{3.52}{\tau_i PRF_i}\right) \tag{18}$$

in the case of a sech^2-shaped pulse. Similarly to Eqs. (13) and (14), the ratio of the erf and/or hyperbolic tangent terms of Eq. (16) are close to 1 for the considered range of duty cycle values (see Tables S2 – S4 in supplement part S3).

The Eq. (16) can be rewritten as:

$$\langle P_1 \rangle \cdot \frac{\sqrt{E_1}}{\sqrt{\delta_1} F_1} = \langle P_2 \rangle \cdot \frac{\sqrt{E_2}}{\sqrt{\delta_2} F_2} \tag{19}$$

relating the mean optical powers at absolute threshold of vision for two lasers of known pulse train parameters. This equation is in fact another form of Eq. (10) and will be valid under assumption that all other factors for both lasers are reasonably the same: wavelength of both sources, beam diameters and their quality, shape of stimulus and way of projecting it on the retina. Moreover, the retinal eccentricity to have the same cone-rod ratio in stimulated area and finally the psychophysical method of finding the threshold. Under such assumptions, the visual threshold measurements performed with one laser allow to empirically determine one side of Eq. (19). Thus the relation:

$$\langle P \rangle = P_{2t} = a \cdot \sqrt{\delta} \cdot \frac{F}{\sqrt{E}} \tag{20}$$

can be established, where mean power P measured by the optical sensor is understood as two-photon visual threshold P_{2t} determined during a given psychophysical procedure and a is a

Biomedical Optics EXPRESS

coefficient that has a physical interpretation as a material constant of the retina, combining the visual threshold P_{2t} with the pulse train parameters.

The expected ratio of the visual threshold values for the two lasers differs, depending only on pulse duration and/or pulse repetition frequency. However, for some applications it may be more suitable to operate on a logarithmic scale, using the two-photon sensitivity S_{2p} values instead of the two-photon visual threshold P_{2t} values [9]:

$$S_{2p} = 10 \log \frac{P_{ref}}{P_{2t}}, \tag{21}$$

where P_{ref} is a reference power level (here – 800 μW). The two-photon sensitivity change ΔS, related to the visual threshold ratio change, equals:

$$\Delta S = S_{2p,2} - S_{2p,1} = 10log \frac{P_{2t,2}}{P_{2t,1}} = -5 \log \frac{\delta_1}{\delta_2}. \tag{22}$$

In other words, regardless of the pulse shape, a ten-fold increase in the duty cycle value is related to the 5 dB drop in two-photon sensitivity S_{2p}.

We want to point out that in the calculations, we considered only two laser pulse temporal profile types – gaussian or sech^2. The reasons are: (1) the laser sources used in the experiments have either gaussian or sech^2 pulse temporal profile, and (2) the analytical calculations are simplified for these cases. However, other pulse shapes may be used in the presented model as it employs integrals over time of the pulse's instantaneous power. Notice that it may change the relationships described in Eqs (12), (15), (16), (19), (20), and (21).

One may wonder how the visual threshold value changes for a pulsed visible stimulus. One-photon (normal) vision is based on the one-photon absorption process, which depends on the light intensity (in contrast to two-photon absorption that depends on the squared light intensity) and utilizes one photon to excite one molecule. Assuming a pulse repetition rate much greater than the critical fusion frequency CFF (the frequency at which a flickering stimulus is perceived as continuous one) [22], the number of excited molecules for the one-photon vision mechanism N^*_{1p} mechanism equals:

$$N^*_{1p}(t) = \phi_{1p} C \sigma_{1p} \frac{\pi}{\lambda^2} \left(\frac{D}{2 f_{eye}} \right)^2 T(\lambda) t_{exp} PRF \int_{-t_1}^{t_1} P_{pulse}(t) dt, \tag{23}$$

where *1p* refers to the one-photon vision mechanism. Similarly to the two-photon vision mechanism, the same number of excited molecules is required to activate the 11-*cis*-retinal in the chromophores. Considering two pulsed visible lasers that differ only in terms of laser pulse train parameters, the difference in the number of absorbed photons is dependent only on the laser pulse repetition frequency and the laser peak power as follows:

$$PRF_1 \int_{-t_1}^{t_1} P_{pulse,1}(t) dt = PRF_2 \int_{-t_2}^{t_2} P_{pulse,2}(t) dt. \tag{24}$$

In such a case, the expected mean power ratio R_{1p} equals:

$$R_{1p} = \frac{\langle P_1 \rangle}{\langle P_2 \rangle} = \frac{t_{exp} \cdot PRF_1 \cdot \int_{-t_1}^{t_1} P_{pulse,1}(t) dt}{t_{exp} \cdot PRF_2 \cdot \int_{-t_2}^{t_2} P_{pulse,2}(t) dt} = \frac{\delta_1 \cdot P_{max,1}}{\delta_2 \cdot P_{max,2}} \cdot \frac{F_1}{F_2}. \tag{25}$$

In other words, the visual threshold for the one-photon vision mechanism depends only on the delivered optical mean power of the incident light. This conclusion is in agreement with the Talbot-Plateau law, which states that a flickering stimulus at frequency above CFF appears identical to a non-flickering (steady) stimulus, if their chromaticity and time-averaged luminance are the same [23].

Biomedical Optics EXPRESS

3. Results

The two-photon visual threshold values measured for various pulse trains are shown in Fig. 3. Because the two-photon sensitivity varies across the retina for the dark-adapted eye [9,14], the two-photon threshold values P_{2t} have been grouped according to the retinal eccentricity. The differences in the retinal sensitivity in the function of the retinal eccentricity at 0, 2.5, and 5 deg may be explained by the differences in the distribution of cones and rods across the retina [24]. The differences in the beam sizes (see Table 2) have been neglected as having a negligible influence on the threshold values in this range [25]. The measurement uncertainty σ_{meas} has three components: the power measurement uncertainty σ_p (±7% that corresponds to ±0.29 dB); the threshold value determination uncertainty σ_{421}, associated with the minimal procedure step (±0.5 dB that corresponds to ±12.2%); and one standard deviation *SD* of the measured threshold values.

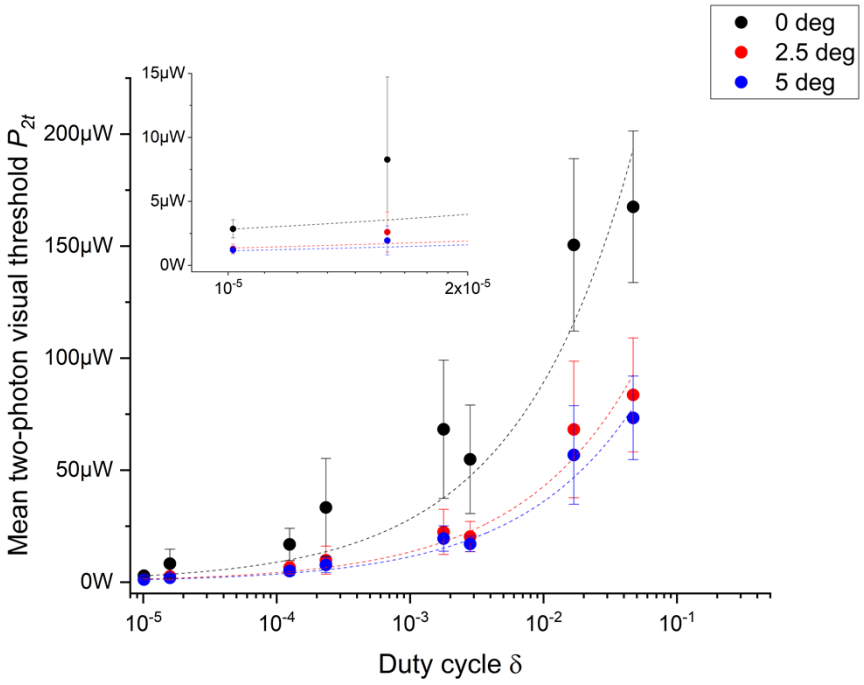

Fig. 3. The measured visual threshold values for various pulse trains. The visual threshold P_{2t} values for 0 deg, 2.5 deg, and 5 deg retinal eccentricity are indicated with black, red, and blue color, respectively. The dots and error bars represent the mean value and measurement uncertainty, respectively. The dashed lines are square root functions ($P_{2t}(\delta) = aE^{-0.5}F\delta^{0.5}$) fitted to the experimental data.

The following equation represents the measurement uncertainty:

$$\sigma_{meas} = \sqrt{\sigma_p^2 + \sigma_{421}^2 + SD^2}. \tag{26}$$

It can be seen that the two-photon visual threshold changes as a function of the duty cycle. The measured values have been compared with the theoretical model. The fitted square root functions for each retinal eccentricity are plotted in Fig. 3 (dashed lines), and the fit coefficients are summarized in Table 3. The shape of the function was chosen based on the theoretical model presented in Section 2.3 (see Eq. (20)). The *a*-coefficient (expressed in Watts) has a physical interpretation of a material constant of the retina that combines the visual threshold

Biomedical Optics EXPRESS

value expressed as mean power value with the pulse train parameters. In other words, it reflects the effectiveness of the two-photon photopigment isomerization for various average power density values (assuming that under constant experimental conditions, the number of photopigment isomerizations required for a visual response is constant). It must be emphasized that the threshold mean power values P_{2t} are in fact the average power levels at the cornea; but as long as the numerical aperture was kept at a similar level for all pulse trains, the values of average power density are proportional to the values of average power at the cornea. The distribution of photoreceptors varies with retinal eccentricity [24], and so does the a-coefficient. The coefficients of determination (COD) of the fit are equal to 0.91, 0.94, and 0.96 for the 0 deg, 2.5 deg, and 5 deg fovea eccentricities, respectively. The COD values close to 1 confirm that the mathematical model fits well the experimental data.

Table 3. Parameters of the fitting curves $f(\delta) = aE^{-0.5}F\delta^{0.5}$ of the visual threshold values measured for various retinal eccentricities. COD is an abbreviation for the coefficient of determination.

Retinal eccentricity	a (value ± standard error)	COD
0 deg	$(7.1 \pm 0.7) \times 10^{-4}$ [W]	0.91
2.5 deg	$(3.3 \pm 0.2) \times 10^{-4}$ [W]	0.94
5 deg	$(2.8 \pm 0.2) \times 10^{-4}$ [W]	0.96

4. Discussion

The results presented in Section 3.1 show that the visual threshold values measured for a two-photon stimulus depend on the laser pulse train parameters, and change as the square root of the duty cycle value. However, potential differences in the retinal spot size of the scanning laser beam, in the spectral properties of the pulse trains, and in the transmittance of the eye medium, even if negligible, were not taken into account. Therefore, the visual thresholds were recalculated to the effective photon density over time N_{eff} – the number of photons per unit time that reach the retina and cause a visual sensation divided by the optotype area at the subject's retina:

$$N_{eff} = P_{2t}\frac{S(\lambda)\cdot T(\lambda)}{E_{ph}(\lambda)\cdot A(\lambda)}, \tag{27}$$

where P_{2t} is the visual threshold power level, $S(\lambda)$ is the normalized spectrum (optical power in the function of wavelength normalized to the unit area) of the pulse train, $E_{ph}(\lambda)$ is the energy of a photon, and $A(\lambda)$ is the stimulated retinal area (ring shaped):

$$A(\lambda) = \pi\left(\left(\frac{StimD + s_{retina}}{2}\right)^2 - \left(\frac{StimD - s_{retina}}{2}\right)^2\right) = \frac{4StimDf_{eye}\lambda}{D}, \tag{28}$$

where $StimD$ is the stimulus diameter size (Goldmann III – 0.5 deg), and s_{retina} is the retinal spot size (diameter), assumed to be a diffraction-limited one:

$$s_{retina} = \frac{4\lambda f_{eye}}{\pi D}. \tag{29}$$

Note, that due to eye aberrations, the real retinal spot size may differ from theoretical calculations. However, for a stimulating beam of diameter 1-2 mm at the cornea, and a normal eye, the impact of these aberrations is not large [26]. The area was calculated based on the equations for the squared illumination point spread function IPSF^2, following Zipfel *et al.* [27], for the central laser wavelength and assuming that 1 deg at the retina corresponds to 288 µm [28].

Biomedical Optics EXPRESS

The effective photon density over time N_{eff} is presented in Fig. 4. The measurement points on the log-log scale are fitted to a linear function with a slope of 0.5, which corresponds to the square root dependence of the change in N_{eff} on duty cycle (see Eqs. (20) and 22 in Section 2.3). The intercept value b (see Table 4) corresponds to the effective photon density over time (photon flux) N_{eff} for an infinitely low duty cycle value. The contribution of the $\log(E^{-0.5}F)$ term has not been excluded from the b coefficient as $\log(E^{-0.5}F) \approx 0.1$ for $\delta \in (0,1$. Such a case may be interpreted as an unrealistic case of infinitely short pulse or infinitely low pulse repetition frequency (Dirac delta). On the other hand, the b value may be interpreted as a boundary value of the photon flux, below which two-photon vision cannot occur. Based on the fit, a constant can be retrieved that links the effective photon flux with the pulse train parameters.

The values presented in Table 4 are retinal material constants (expressed as $\log(\text{photons}\cdot\text{s}^{-1}\cdot\text{m}^{-2})$) that correspond to the photon flux at the retina required to achieve the two-photon visual threshold stimulus. Referring to the equations presented in the Section 2.3, this constant corresponds to all the factors associated with the optical properties of the human eye, including the transmittance of the eye medium and the numerical aperture of the eye. The effective values of photon density over time N_{eff} for two-photon vision can be related to those observed for one-photon vision determined in similar stimulating conditions and psychophysical procedures. For example, for a 520.7-nm visible green stimulus and a 1.2 mm $1/e^2$ beam diameter size, the N_{eff} value corresponding to the visual threshold is 12.1 ± 0.1 $\log(\text{phot}\cdot\text{s}^{-1}\cdot\text{m}^{-2})$: mean value for 3 healthy subjects at fovea center, 5 trials for each subject [11]. For experiments described in Ruminski *et al.* [14], the visual threshold value for the fovea center is below 1 pW (approx. 0.75 pW, see Fig. 3 a) in [14]), which after taking into account beam size gives a $\log(N_{eff})$ value of ~11.7 $\log(\text{phot}\cdot\text{s}^{-1}\cdot\text{m}^{-2})$: for 1 subject. Thus, two-photon vision requires ~10 orders of magnitude higher photon flux to be perceived by a dark-adapted subject (compared with sub-picosecond NIR lasers used in the experiments described in this paper; see black data points in Fig. 4 that takes $\log(N_{eff})$ values 21-23 $\log(\text{phot}\cdot\text{s}^{-1}\cdot\text{m}^{-2})$). Note, that for one-photon vision, the N_{eff} value does not depend on the duty cycle.

Table 4. Parameters of the fitting curves $f = 0.5x + b$ of the calculated logarithm of the effective photon flux N_{eff} values for various retinal eccentricities. COD is an abbreviation for the coefficient of determination.

Retinal eccentricity	b (value ± standard error)	COD
0 deg	24.23 ± 0.05 [$\log(\text{photon}\cdot\text{s}^{-1}\cdot\text{m}^{-2})$]	0.96
2.5 deg	23.90 ± 0.03 [$\log(\text{photon}\cdot\text{s}^{-1}\cdot\text{m}^{-2})$]	0.99
5 deg	23.83 ± 0.02 [$\log(\text{photon}\cdot\text{s}^{-1}\cdot\text{m}^{-2})$]	0.99

The magnitudes of the coefficients a and b listed in Tables 3 and 4 are specific to the dark-adapted retina – represent detection threshold. Those found for the central location will be characteristic of the cones due to the lack of rods in the macula's central part. Those of 5 deg will characterize a mixture of types, presumably with the more prominent contribution of rods, because of their higher sensitivity in a dark-adapted state. The model could also be applied to light-adapted conditions, but separate measurements will be required to determine the magnitude of the coefficients a and b under such conditions.

This paper presents the visual threshold values measured for a selected set of values of pulse duration and pulse repetition frequency. One may wonder if a particular pulsed NIR laser (with different pulse train parameters than those presented in this work) may or may not be perceived *via* the two-photon vision mechanism. This can be assessed using the mathematical model presented in Section 2.3, along with coefficients from Table 3. In the following part of this section, we will provide an example of analysis of the visibility of a pulsed NIR laser. Note that this analysis does not consider factors such as substantially different beam sizes that would alter

Biomedical Optics EXPRESS

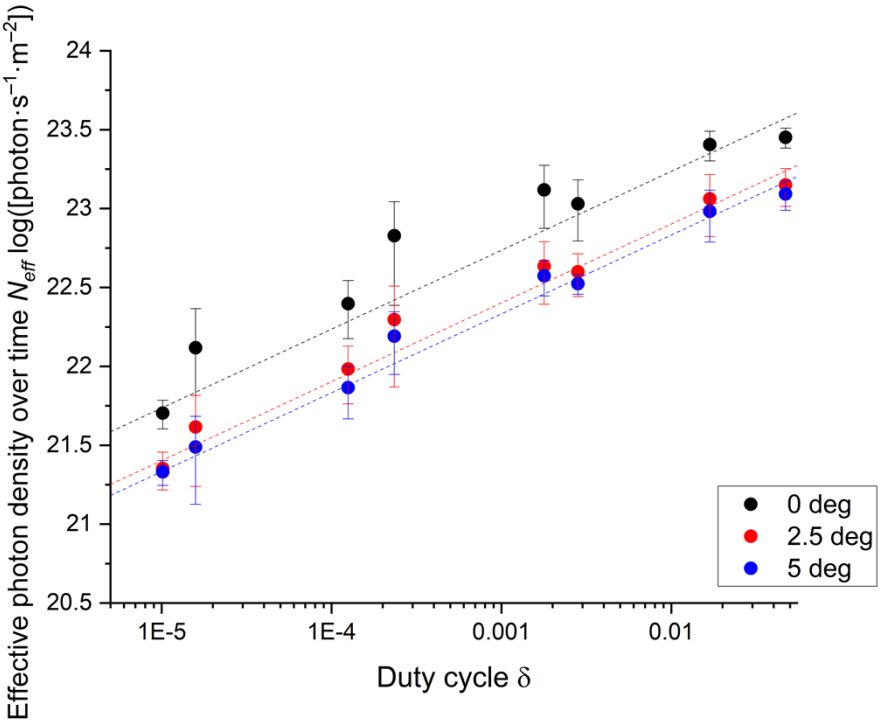

Fig. 4. The effective photon flux N_{eff} for various pulse trains. The effective photon density N_{eff} values for retinal eccentricity values of 0 deg, 2.5 deg, and 5 deg are indicated with black, red, and blue colors, respectively. The dots and error bars correspond to the mean value and measurement uncertainty. The dashed lines are the linear fit functions with a slope of 0.5.

the effective photon density at the retina [25], or laser wavelength, which may affect sensitivity, as the sensitivity of the human retina varies with stimulus wavelength [11,29].

In this example, let us consider a Ti:sapphire laser emitting sech^2 pulses at 1030 nm with a pulse repetition frequency of 80 MHz for a two-photon vision application. As the pulse duration may be altered by stretching the pulse, let us check how long pulses could be perceived by the two-photon vision mechanism. The simulation outcome is presented in Fig. 5 a). For each data point, the duty cycle value and the expected threshold value have been calculated. One may see that the expected threshold value increases as a function of the duty cycle. For safe illumination with a stationary beam for 1 hour, the Maximum Permissible Radiant Power (MPΦ) level has been calculated as 409 μW [18]. MPΦ level is plotted in Fig. 5 a) as the red line; and the red cross-hatched area represents expected values of mean power level that exceed safe illumination conditions. Note that the ANSI standard does not specify directly MPΦ for pulses shorter than 100 fs. For this simulation, the MPΦ levels are equal to the threshold values for 2.5-ns or 11.3-ns pulses, and at the fovea center or at a 2.5 foveal eccentricity, respectively. In other words, pulses shorter than 2.5 ns or 11.3 ns should be perceived by a dark-adapted observer if the stimuli are presented at the fovea center or 2.5 deg foveal eccentricity. For 5 deg foveal eccentricities, even continuous-wave radiation (duty cycle of 1) should be visible for the observer due to two-photon process.

Next, let us consider another situation – a laser emitting sech^2 1 ps-long pulses at 1030 nm. The simulation outcome is presented in Fig. 5 b). Once again, for each data point, the duty cycle value and the expected threshold value have been calculated. Similarly to Fig. 5 a), the

Biomedical Optics EXPRESS

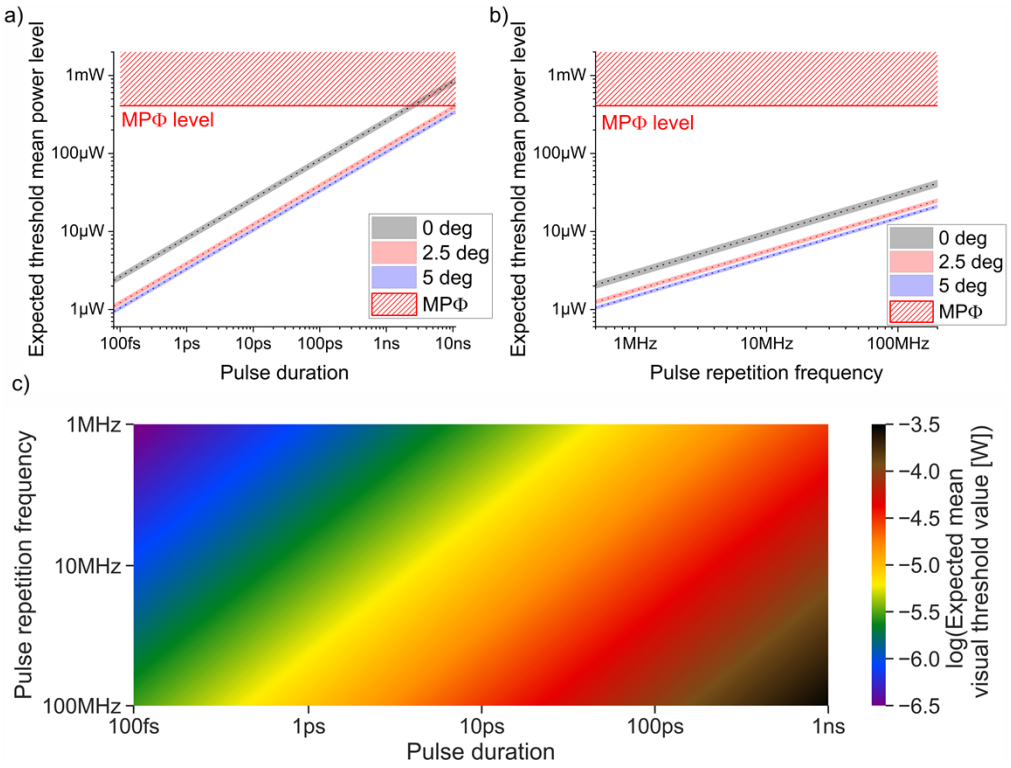

Fig. 5. The expected mean threshold power level for the two-photon vision mechanism. Simulations for a 1030-nm laser operating at: a) 80 MHz pulse repetition rate (Ti:sapphire), b) 1-ps pulse duration. The values for 0, 2.5, and 5 deg are represented with black, red, and blue colors, respectively. The vertical lines show simulated points and are connected with dotted lines. The shaded color represents the expected threshold value uncertainty (one standard error). The horizontal red line represents the MPΦ level for 1-hour exposure for a stationary beam (409 μW), and the cross-hatched area above corresponds to hazardous power levels. c) The expected mean visual threshold value at the fovea center for a pulsed laser operating at 1030 nm. The visual threshold values are indicated with various colors. See also an animated version of this figure in Python: https://github.com/mmarze/2phVisThreshold.git

expected threshold value level increases as a function of the duty cycle. Note that for pulse repetition frequencies ranging from 1 MHz to 100 MHz, the expected visual threshold values are significantly below the MPΦ level.

Analogous calculations can be performed for various pulse-train parameter values. Figure 5 c) presents the simulation of a mean visual threshold value level at the retina center (retinal eccentricity of 0 deg) for a pulsed laser emitting at 1030 nm, pulse duration in the range from 100 fs to 1 ns, and *PRF* in the range from 1 MHz to 100 MHz. Notice that laser sources operating at low pulse repetition rates enable perception of a relatively bright two-photon stimulus (the expected visual threshold value is the lowest). The MPΦ level corresponds to $\log(409 \times 10^{-6}$ W) = –3.4 log(W). The graphs presented in Fig. 5 show that two-photon visibility of pulsed lasers of wavelength ~1000 nm cover 3 orders of magnitude of stimulating beam power.

The data presented in Fig. 5 can be used also for a rough estimation of the two-photon brightness of pulsed lasers in the investigated spectral range. For example, an analysis for the Ti:sapphire laser (λ_c = 1030 nm, *PRF* = 80 MHz, sech^2 pulse; see Fig. 5 a)) is as follows: the available brightness range results from the range between the visual threshold and the MPΦ level;

Biomedical Optics EXPRESS

e.g., 8 μW to 409 μW for a 1-ps pulse at the fovea center. As reported by Ruminski *et al.* [14], so the relative change of the stimulus power level (*e.g.*, two-times) would changes the brightness of a two-photon stimulus quadratically as compared to one-photon vision (*e.g.*, four times, see Fig. 3 b) in [14]). Therefore, if the MPΦ level is ~51 times higher than the expected threshold level, we could expect the available brightness range for the one-photon vision mechanism to be ~2600 times higher than the visual threshold (from ~20 fW to ~52 pW).

5. Conclusions

In this paper, we presented a practical tool for evaluating a pulsed NIR laser for two-photon vision applications. We presented the results of psychophysical experiments performed for pulse trains of which duty cycle parameters cover a range of over three orders of magnitude. All of the experimental factors regarding the stimulating pulsed laser were carefully measured and fully controlled during the experiments. Moreover, we derived a mathematical model that combines the pulse train parameters (pulse duration, pulse repetition frequency, and pulse shape) with the visual threshold value, and found good agreement with our experimental data. We also demonstrated how to use the model with particular data to predict the visual threshold of any pulsed NIR laser and the corresponding available brightness range.

This work is expected to be of interest for laser engineers, as it enables tuning of the pulsed NIR laser parameters to optimize them for two-photon applications. It should also attract the attention of the community interested in nonlinear visual perception. Further, it may contribute to the development of two-photon vision-based ophthalmic devices for ophthalmic diagnostics [9,14]; or a new generation of two-photon driven displays (*e.g.* retinal projectors), which are emerging as interesting tools for virtual reality (VR) and augmented reality (AR) applications.

Funding. Fundacja na rzecz Nauki Polskiej (MAB/2019/12).

Acknowledgments. The International Centre for Translational Eye Research (MAB/2019/12) project is carried out within the International Research Agendas programme of the Foundation for Polish Science co-financed by the European Union under the European Regional Development Fund.

We would like to thank Yuriy Stepanenko, Ph.D., for a loan of a fast photodiode and a wideband oscilloscope for long pulse duration measurements.

Disclosures. The authors declare no conflicts of interest.

Data availability. Data underlying the results presented in this paper are not publicly available at this time but may be obtained from the authors upon reasonable request.

Supplemental document. See Supplement 1 for supporting content.

References

1. A. Valberg, "Light," in *Light, Vision, Color* (John Wiley & Sons, Ltd, 2005), pp. 35–39.
2. C. F. Goodeve, "Vision in the Ultra-Violet," Nature **134**(3385), 416–417 (1934).
3. C. F. Goodeve, "Relative Luminosity in the Extreme Red," Proc. R. Soc. London. Ser. A - Math. Phys. Sci. **155**(886), 664–683 (1936).
4. D. R. Griffin, R. Hubbard, and G. Wald, "The sensitivity of the human eye to infra-red radiation," J. Opt. Soc. Am. **37**(7), 546–554 (1947).
5. L. S. Vasilenko, V. P. Chebotaev, and Y. V. Troitskii, "Visual Observation of Infrared Laser Emission," J. Expreminetal Theor. Phys. **48**(3), 777–778 (1965).
6. D. H. Sliney, R. T. Wangemann, J. K. Franks, and M. L. Wolbarsht, "Visual Sensitivity of the Eye To Infrared Laser Radiation," J. Opt. Soc. Am. **66**(4), 339–341 (1976).
7. V. G. Dmitriev, V. N. Emel'yanov, M. A. Kashintsev, V. V Kulikov, A. A. Solov'ev, M. F. Stel'makh, and O. B. Cherednichenko, "Nonlinear perception of infrared radiation in the 800–1355 nm range with human eye," Sov. J. Quantum Electron. **9**(4), 475–479 (1979).
8. G. Palczewska, F. Vinberg, P. Stremplewski, M. P. Bircher, D. Salom, K. Komar, J. Zhang, M. Cascella, M. Wojtkowski, V. J. Kefalov, and K. Palczewski, "Human infrared vision is triggered by two-photon chromophore isomerization," Proc. Natl. Acad. Sci. U. S. A. **111**(50), E5445–E5454 (2014).
9. M. J. Marzejon, Ł. Kornaszewski, J. Bogusławski, P. Ciąćka, M. Martynow, G. Palczewska, S. Maćkowski, K. Palczewski, M. Wojtkowski, and K. Komar, "Two-photon microperimetry with picosecond pulses," Biomed. Opt. Express **12**(1), 462–479 (2021).

Biomedical Optics EXPRESS

10. A. Zielinska, P. Ciaćka, M. Szkulmowski, and K. Komar, "Pupillary Light Reflex Induced by Two-Photon Vision," Investig. Ophthalmol. Vis. Sci. **62**(15), 23 (2021).
11. D. Stachowiak, M. Marzejon, J. Bogusławski, Z. Łaszczych, K. Komar, M. Wojtkowski, and G. Soboń, "Femtosecond Er-doped fiber laser source tunable from 872 to 1075 nm for two-photon vision studies in humans," Biomed. Opt. Express **13**(4), 1899–1911 (2022).
12. G. Łabuz, A. Zielińska, L. J. Kessler, A. Rayamajhi, K. Komar, R. Khoramnia, and G. U. Auffarth, "Two-Photon Vision in Age-Related Macular Degeneration: A Translational Study," Diagnostics **12**(3), 760 (2022).
13. P. Artal, S. Manzanera, K. Komar, A. Gambín-Regadera, and M. Wojtkowski, "Visual acuity in two-photon infrared vision," Optica **4**(12), 1488–1491 (2017).
14. D. Ruminski, G. Palczewska, M. Nowakowski, A. Zielińska, V. J. Kefalov, K. Komar, K. Palczewski, and M. Wojtkowski, "Two-photon microperimetry: sensitivity of human photoreceptors to infrared light," Biomed. Opt. Express **10**(9), 4551–4567 (2019).
15. S. Manzanera, D. Sola, N. Khalifa, and P. Artal, "Vision with pulsed infrared light is mediated by nonlinear optical processes," Biomed. Opt. Express **11**(10), 5603–5617 (2020).
16. M. Marzejon, Ł. Kornaszewski, M. Wojtkowski, and K. Komar, "Effects of laser pulse duration in two-photon vision threshold measurements," in *Ophthalmic Technologies XXXI*, D. X. Hammer, K. M. Joos, and D. V Palanker, eds. (SPIE, 2021), **11623**, pp. 74–79.
17. G. Westheimer, "Directional sensitivity of the retina: 75 Years of Stiles-Crawford effect," Proc. R. Soc. B Biol. Sci. **275**(1653), 2777–2786 (2008).
18. American National Standard Institute*, American National Standard for Safe Use of Lasers (ANSI Z136.1-2014)* (2014).
19. C. Xu and W. W. Webb, "Measurement of two-photon excitation cross sections of molecular fluorophores with data from 690 to 1050 nm," J. Opt. Soc. Am. B **13**(3), 481–491 (1996).
20. H. Gross, F. Blechinger, and B. Achtner, "Human Eye," in *Handbook of Optical Systems*, (Wiley Online Books, 2008), pp. 1–87.
21. L. C. Andrews, *Special Functions of Mathematics for Engineers*, 2nd ed. (SPIE, 1998).
22. D. H. Kelly, "Visual Responses to Time-Dependent Stimuli.* I. Amplitude Sensitivity Measurements†," J. Opt. Soc. Am. **51**(4), 422–429 (1961).
23. A. M. McKendrick and C. A. Johnson, "Temporal Properties of Vision," in *Adler's Physiology of the Eye*, P. L. Kaufman and A. Alm, eds., 11th ed. (Mosby International, 2011), pp. 698–712.
24. A. Valberg, "The retina," in *Light, Vision, Color* (John Wiley & Sons, Ltd, 2005), pp. 98–110.
25. K. Komar, A. Zielinska, P. Ciacka, D. Ruminski, M. Szkulmowski, and M. Wojtkowski, "Effect of stimulating beam diameter on two-photon visual thresholds," Invest. Ophthalmol. Vis. Sci. **63**(7), 2233 (2022).
26. A. Roorda, "Adaptive optics for studying visual function: A comprehensive review," J. Vis. **11**(5), 6 (2011).
27. W. R. Zipfel, R. M. Williams, and W. W. Webb, "Nonlinear magic: Multiphoton microscopy in the biosciences," Nat. Biotechnol. **21**(11), 1369–1377 (2003).
28. N. Drasdo and C. W. Fowler, "Non-linear projection of the retinal image in a wide-angle schematic eye," Br. J. Ophthalmol. **58**(8), 709–714 (1974).
29. M. Marzejon, A. Zielinska, D. Stachowiak, G. Sobon, M. Wojtkowski, and K. Komar, "Towards spectral sensitivity curve for two-photon vision mechanism," Invest. Ophthalmol. Vis. Sci. **63**(7), 2232 (2022).